Determination of the electron temperature and density in the negative glow of a nitrogen pulsed discharge using optical emission spectroscopy

2010 J. Phys. D: Appl. Phys. 43 015202

(http://iopscience.iop.org/0022-3727/43/1/015202)

J. Phys. D: Appl. Phys. **43** (2010) 015202 (10pp) doi:10.1088/0022-3727/43/1/015202

Determination of the electron temperature and density in the negative glow of a nitrogen pulsed discharge using optical emission spectroscopy

L M Isola[1], B J Gómez[1] and V Guerra[2]

[1] Instituto de Física Rosario (CONICET-UNR), Febrero 210 Bis., 2000 Rosario, Argentina
[2] Centro de Física dos Plasmas Instituto Superior Técnico 1049-001 Lisboa, Portugal

Received 10 July 2009, in final form 25 October 2009
Published 7 December 2009
Online at stacks.iop.org/JPhysD/43/015202

Abstract
A new method for experimentally determining the electron density (n_e) and the electron temperature (T_e) in the negative glow of a nitrogen pulsed discharge is presented. It is based on optical emission spectroscopy (OES) and consists of a variation and refinement of relatively similar schemes previously reported for different working conditions by other authors. The bottom line is the measurement of the emission intensities of the (0,0) bands of the first negative system at 391.44 nm and of the (0,2) bands of the second positive system at 380.49 nm.
The suggested procedure allows the establishment of the absolute values of n_e and T_e, as long as one calibration point is provided, such as the electron density at one specific discharge condition. If this calibration point is unavailable, the method nonetheless yields a qualitative dependence of T_e and n_e. Langmuir probe measurements confirm and validate the OES results for n_e, thereby legitimizing the diagnostic technique developed. The interpretation of the results for T_e is slightly more complex, and in some circumstances an accurate determination of T_e may require further analysis.

1. Introduction

Nitrogen containing discharges are extensively used in several plasma processing techniques, such as the surface modification of different materials [1–3]. They also play a very important role in the study of atmospheric chemistry and different environmental problems, such as the investigation of the NO_x and O_3 production and destruction mechanisms [4, 5] or the research on low-temperature plasma sterilization [6, 7]. Moreover, in a number of plasma processes the samples must often be placed on the cathode, whereas the use of pulsed plasmas has the advantage of avoiding damages by arc, and allows us to monitor the sample heating by pulse control [8, 9]. The study of the negative glow of pulsed nitrogen discharges thus becomes of importance.

Optical emission spectroscopy (OES) is a non-intrusive and relatively easy-to-use procedure, which makes it widely applicable to characterize these nitrogen plasmas [8–15]. However, due to the complexity and variety of discharge conditions, most papers that can be found in the literature using OES provide essentially qualitative analyses. Herein OES is used together with a simple kinetic description of the discharge in order to obtain quantitatively the electron temperature, T_e, and the electron density, n_e, in the negative glow of a nitrogen pulsed discharge operating at pressures in the range 2–4 Torr. In particular, T_e and n_e are derived from the emission intensities of the (0, 0) band of the first negative system (1^-) at 391.44 nm, I^+_{BX}, to the (0, 2) band of the second positive system (2^+) at 380.49 nm, I_{CB}. The OES results are then compared with independent Langmuir probe measurements.

The idea of using the emission intensities to investigate nitrogen discharges is not new. For instance, in [16] the ratio of the bands from the first negative system $N_2^+(0–0)$ at 391.44 nm and from the second positive system $N_2(2–5)$ at 394.30 nm was used to estimate the electronic temperature in a RF discharge. The details of the method are described in [11]. The procedure

from [16] can be used if the level $N_2(C\,^3\Pi_u)$ is predominantly excited by electron collisions with ground state $N_2(X\,^1\Sigma_g^+)$ molecules, and if the ionic state $N_2^+(B\,^2\Sigma_u^+)$ is mainly excited by electrons from the ground state of the neutral molecule $N_2(X\,^1\Sigma_g^+)$.

Clearly, the actual excitation mechanism of $N_2^+(B\,^2\Sigma_u^+)$ in a specific discharge may call for modifications of the methodology. Britun *et al* [16] argue, following [17], that for the conditions of their investigation only the excitation of $N_2^+(B\,^2\Sigma_u^+)$ from ground state neutral molecules is relevant, the method being thus usable in a straightforward way. Nevertheless, a plasma column of a stationary dc glow discharge was studied in [18], where it was inferred, in contrast, that the excitation of $N_2^+(B\,^2\Sigma_u^+)$ takes place by electron collisions with ground state ions, $N_2^+(X\,^2\Sigma_g^+)$. In addition, in another study of a positive column of a dc discharge [19], collisions involving ground state ions and vibrationally excited molecules $N_2(X\,^1\Sigma_g^+,\ v > 12)$,

$$N_2^+(X) + N_2(X, v > 12) \rightarrow N_2^+(B) + N_2(X, v - 12), \qquad (1)$$

were identified as the most important mechanism of formation of the radiative ionic state. The different conclusions from [16, 18, 19] sharply indicate that extreme care must be taken in using the ratio of emission bands as a diagnostic tool, as the processes involved in the creation of the emitting states vary with the particular conditions of operation of each discharge.

An additional point of concern is the possible influence of the metastable state $N_2(A\,\Sigma_u^+)$ in the population of $N_2(C\,\Pi_u)$ [8, 13, 15, 20–24]. For instance, a detailed analysis of the discharge kinetics with a self-consistent calculation of the electron energy distribution function (EEDF) was made in [22] both for the positive column of a dc discharge and for a surface-wave sustained discharge, where the contribution of the pooling reaction

$$N_2(A) + N_2(A) \rightarrow N_2(C) + N_2(X, v = 2) \qquad (2)$$

to the excitation of $N_2(C\,\Pi_u)$ was pointed out.

Another idea to use the ratio of nitrogen emission bands was presented in [23], where it was suggested that the electron temperature can be determined in an ICP discharge from the ratio of the 2^+ to the first positive 1^+ intensities, I_{CB}/I_{BA}. In spite of the good results obtained for the conditions studied in [23], the method has several drawbacks. As a matter of fact, it needs the determination of the total intensity emission of the 1^+ and 2^+ systems, and not only of two particular transitions. This implies an additional experimental complexity, and the prerequisite of having the same spectral response in the complete range of wavelengths to be observed. Furthermore, it requires an independent determination of n_e. Finally, the model did not take into account the pooling reactions (2). This was corrected in a later work [25], which included the effect of these reactions.

A variant of the same idea was developed in [26], the average electron density in an ICP being determined from the emission intensity ratio of the $N_2(1, 3)$ (375.5 nm) and $N_2(0, 0)$ (337.1 nm) bands of the second positive system. However, the method requires an independent determination of the electron temperature of low energy electrons, which is difficult to obtain when the EEDF deviates from a Maxwellian. In addition, the underlying model does not consider the pooling reactions and needs a strong variation of the ratio of the bands involved, which is not always the case.

Note that all the works referred to above are based on the ratio of emission bands and do not provide as much information as the method suggested in this work. Actually, the latter uses directly the emission bands instead of their ratio, allowing the determination of the qualitative dependence of T_e and n_e. These can even be obtained in absolute value, provided a calibration point is available.

The structure of this paper is as follows. Section 2 briefly describes the experimental set-up both for the OES and for the Langmuir probe measurements. The proposed method is detailed in section 3, a critical discussion of its applicability being presented in the subsequent section. The experimental results are given in section 5, as part of a study of the negative glow of a nitrogen pulsed discharge. Finally, section 6 summarizes the main results and concludes the paper.

2. Experimental set-up

The plasma reactor used in this work consists of a stainless-steel chamber 254 mm in diameter and 360 mm in height, with two side glass windows. The experimental set-up is schematically shown in figure 1. The work pressure ranged from 2 to 4 Torr, which are typical values used in surface treatment, and the gas flow rate was kept constant at 92 ml min^{-1}. The discharge was generated between a central disc, on which the sample to be treated is placed and which works as a cathode, and the walls of the chamber. A variable pulsed source with a frequency of 200 Hz and a duty cycle of 0.7 was used, keeping the voltage constant at −630 V. The discharge current changes from 0.455 A at 2.00 Torr to 0.850 A at 3.80 Torr. The operating conditions are detailed in table 1.

The optical emission spectra from the discharge were recorded with a Jarrell–Ash monochromator with Czerney–Turner mounting. The slit entry was set at 25 μm, whereas the grating used was 1200 grooves mm^{-1}. A lens focused the light to the monochromator, and a linear arrangement of 1024 photodiodes was used as the detector. A laser was used to align the system and the input slit was reduced vertically in order to ensure the observation of a small area of the discharge, typically of the dimensions of the region characterized by the Langmuir probe. This makes the comparison between the OES and the probe measurements more meaningful and valuable.

Concerning the probe measurements, a cylindrical Langmuir probe consisting of a tungsten wire of radius $R = 15\ \mu$m and length $L = 60$ mm was employed. It was fed by a 0–40 V variable source, synchronized with the pulsed plasma source as to apply the voltage in the last millisecond of each cycle.

To measure the probe characteristic we used a SR-250 and Boxcar Averaging Gaiter Integrated module, averaging over 200 current measurement sets, 800 μs after the application of voltage in the probe. This voltage is measured with the

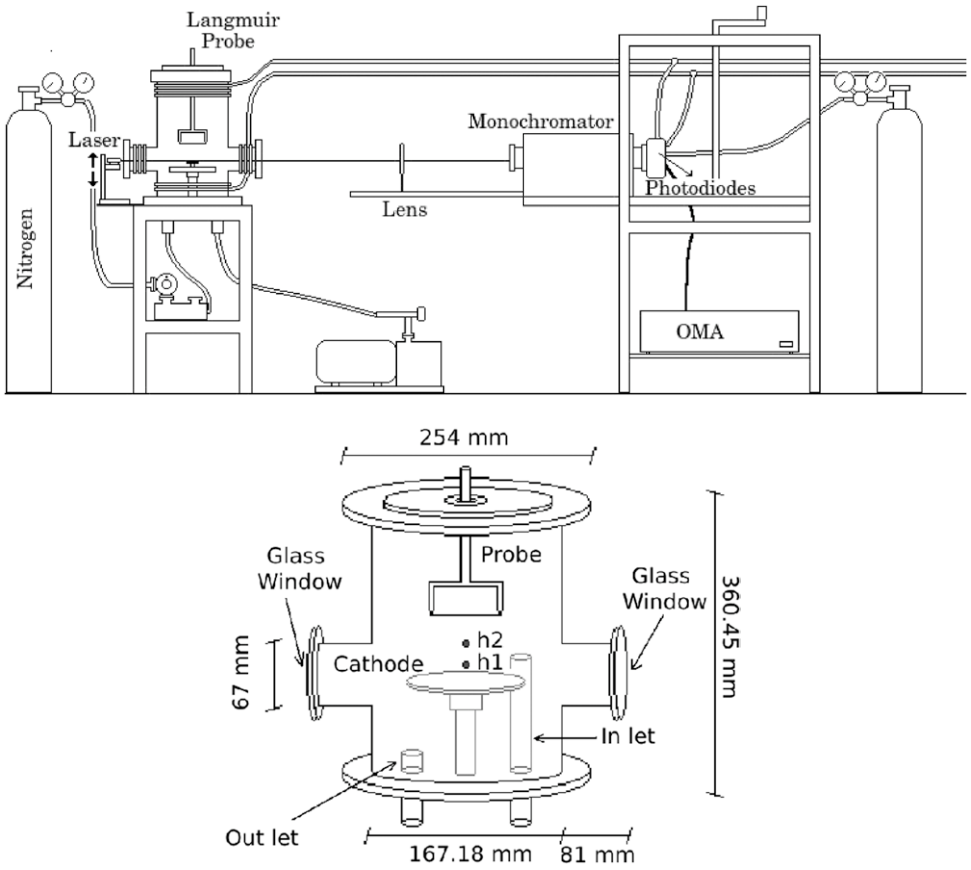

Figure 1. Experimental set-up.

Table 1. Discharge parameters.

Pressure (Torr)	Current (A)
2.00	0.455
2.20	0.525
2.40	0.570
2.60	0.620
2.80	0.660
3.00	0.700
3.20	0.750
3.40	0.770
3.60	0.810
3.80	0.850

interface of the module SR-245, and a numerical averaging over 20 data sets is performed.

Note that to carry out measurements with an electric probe we need to know the probe operation regime. A complete review of the different operation regimes and their theoretical description is available in [27]. For our discharge conditions, the following condition is verified:

$$\lambda_e \geqslant \frac{3R}{4} \ln\left(\frac{\pi L}{4R}\right), \tag{3}$$

where λ_e is the electron mean free path ($\lambda_e \gtrsim 160\,\mu$m). Note that the pressure influence on the probe operation regime is included in the electrons mean free path λ_e. Then as the condition of equation (3) is verified, our probe operation regime is non-collisional, i.e. there are no collisions in the region disturbed by the probe and the Druyvesteyn method can be applied. Besides, we have not observed any perturbation arising from the probe in the discharge electrical parameters. The EEDF $g(\varepsilon)$ can then be obtained from the second derivative of the probe characteristic,

$$g_e(\varepsilon) = \frac{2m}{e^2 A}\left(\frac{2\varepsilon V}{m}\right)^{\frac{1}{2}} \frac{d^2 I_e}{dV^2}, \tag{4}$$

where ε denotes the electron energy, m is the electron mass, V is the probe voltage with respect to the plasma potential, A is the area of the probe and the maximum of the first derivative has been taken as the plasma potential.

The electron density and effective temperature are then obtained from

$$n_e = \int_0^\infty g_e(\varepsilon)\, d\varepsilon \tag{5}$$

and

$$\langle\varepsilon\rangle = \frac{1}{n_e}\int_0^\infty \varepsilon g_e(\varepsilon)\, d\varepsilon = \frac{3}{2}T_{\text{eff}}. \tag{6}$$

Both the OES and the Langmuir probe measurements were carried out at two different positions in the discharge chamber, marked in figure 1 by h_1 and h_2, h_1 being closer to the cathode, $h_1 = 6$ mm and $h_2 = 18$ mm.

3. The diagnostic method

3.1. Principles and methodology

In this work we propose a new method to determine the electron temperature and density in the negative glow of a nitrogen pulsed discharge. The technique is based on a simple model for the kinetics of the negative glow, described by the following assumptions:

- nitrogen molecules in the ground state $N_2(X, v = 0)$ constitute the dominant species;
- there is charge neutrality and the primary ion is N_2^+;
- the EEDF is Maxwellian;
- the main reaction of excitation of state $N_2(C, v')$ is

$$e + N_2(X, 0) \rightarrow e + N_2(C, v'); \tag{7}$$

- the $N_2^+(B, v')$ ionic state is essentially produced by the electron impact processes

$$e + N_2(X, 0) \rightarrow e + e + N_2^+(B, v'), \tag{8}$$

$$e + N_2^+(X, 0) \rightarrow e + N_2^+(B, v'); \tag{9}$$

- levels $N_2(C, v')$ and $N_2^+(B, v')$ are primary lost by radiative decay.

If these conditions are fulfilled, the intensity of the head band of the second positive system of nitrogen for a particular transition (C, v')–(B, v'') is given by

$$I_{CB}(v', v'') = K_{CB}(\lambda_{CB}) n_0 n_e \langle \sigma_X^C v_e \rangle \frac{A_{CB}(v', v'')}{\sum_{v''} A_{CB}(v', v'')}, \tag{10}$$

where n_0 denotes the density of nitrogen molecules in the ground state with $v = 0$, n_e the electron density, σ_X^C the excitation cross section of process (7), v_e the electron speed, A_{ij} the relevant Einstein coefficients and $K_{CB}(\lambda_{CB})$ the spectral response of the monochromator at wavelength λ_{CB}.

Similarly, for the emission intensity of the first negative system N_2^+, and considering the two mechanisms (8) and (9), we have

$$I_{BX}^+(v', v'') = K_{BX}^+(\lambda_{BX}^+)(n_0 n_e \langle \sigma_X^{B+} v_e \rangle + n_e^2 \langle \sigma_{X+}^{B+} v_e \rangle) \frac{A_{BX}^+(v', v'')}{\sum_{v''} A_{BX}^+(v', v'')}, \tag{11}$$

where $\sigma_X^{B^+}$ and $\sigma_{X^+}^{B^+}$ are the collision excitation cross sections of mechanisms (8) and (9), respectively.

In equations (10) and (11) there are *a priori* four unknowns, namely, the electron density, n_e, the electron temperature of the Maxwellian distribution, T_e, and the spectral responses of the monochromator, $K_{CB}(\lambda_{CB})$ and $K_{BX}^+(\lambda_{BX}^+)$, which will be equal if we choose two transitions with very close wavelengths. In this case, note that $K \simeq K_{CB} \simeq K_{BX}^+$ is independent of the discharge parameters. Hence, if it is possible to have an initial condition, such as the electron density or the electron temperature for one given situation, the value of K can be obtained. Consequently, T_e and n_e can then be inferred for all other conditions simply by solving a system of two equations with two unknowns. In practice, this corresponds to have a calibration point, and there are no restrictions on the choice of the conditions used to perform it. If, on the other hand, it is not possible to obtain the value of K, the present scheme still allows the determination of the relative dependence of the electron density and the electron temperature on the discharge operating parameters.

Herein we apply the method using the transitions $I_{CB}(0, 2)$ at 380.49 nm and $I_{BX}^+(0, 0)$ at 391.44 nm. These transitions are relatively close in wavelength and their intensities are sensitive to the discharge operating conditions of interest in this study.

The kinetic model proposed here does not include the influence of N atoms, because in this region of the discharge its density is very low compared with N_2. Therefore, their effects in the overall kinetics are not essential. This was in fact confirmed experimentally, as there are not intense atomic lines of nitrogen in the OES measured spectrum.

3.2. Collisional data

There are two recent compilations of cross sections for the collisions between electrons and nitrogen molecules, by Itikawa [28] and by Tabata *et al* [29]. The latter also proposes recommended interpolations for the different cross sections, and is used as a basis in this paper.

3.2.1. Excitation cross section of level $N_2(C\,^3\Pi_u, v' = 0)$. As discussed in [28], the excitation cross section σ^{Exc} of the electronic level $C\,^3\Pi_u$ from the ground state was determined in [30, 31] by beam experiments. Subsequently, and using these works together with two sets of beam measurements [32, 33] and a swarm experiment [34], Brunger *et al* [35] have determined the best values of the excitation cross section, with an estimated uncertainty of 30%. Tabata *et al* [29] also cite additional work [36], which is in good agreement with the previous ones.

As for the emission cross section σ^{Emis} of the second positive system ($C\,^3\Pi_u \rightarrow B\,^3\Pi_g$), it was also reported by several groups. Zubek [37] measured the band (0, 0) (337.13 nm) over electron energies from threshold to 17.5 eV and used a previous measurement of the maximum value of the cross section (11.28×10^{-18} cm^2 at 14.1 eV) to normalize it. Shemansky *et al* [38] measured the bands (0, 0) (337.13 nm) and (1, 0) (315.93 nm) in the energy range 11.23–40.4 eV and extrapolated their measured values with an analytical formula above 300 eV. They normalized their cross section from the emission cross section of the first negative system measured by Borst and Zipf [39]. In a subsequent work, Doering and Yang [40] used an (e,2e) method and determined a better value for the first negative emission cross section at 391.4 nm, which was 14.8% lower. That being so, the value of Shemansky [38] may have to be reduced in the same proportion.

Finally, Fons *et al* measured the emission cross section of second positive system even above 600 eV [41]. Their measurements match to the work of Shemansky without renormalization.

The interpolation formula given in [29] includes the experimental measurements of σ^{Emis} cited above, included [38] without renormalization. As the reported cross sections agree very well, the expressions proposed in [29] are used in this

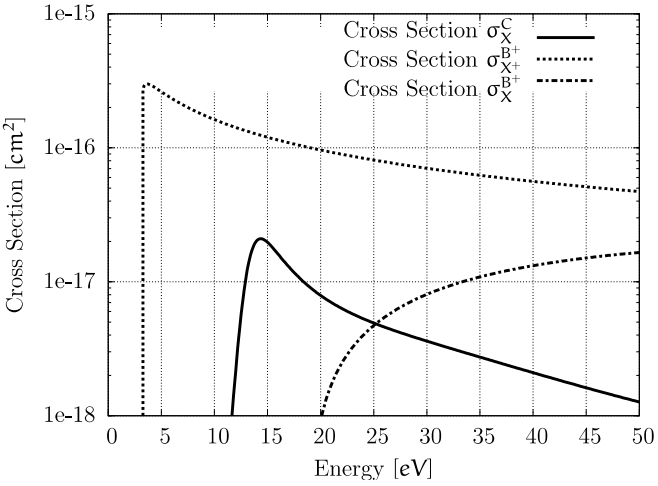

Figure 2. Electron impact cross sections used in this work: (——) σ_X^C, (· · · · · ·) σ_X^{B+}, (— · —) σ_{X+}^{B+}.

paper. Figure 2 depicts the final cross section σ_X^C herein considered, together with the other cross sections required to analyse our experimental data (detailed below).

It is still worth noting that if the excitation cross section σ_X^C is calculated from the emission cross section at 337.13 nm ($\sigma_{0\to0}^{Emis} = \sigma_X^C A_{CB}(0,0)/\Sigma_{v''} A_{CB}(0,v'')$), as done in [29] and used here, it differs from the one obtained from energy loss measurements the former being a factor of about 1.5 lower [28]. However, since we are using the cross sections to analyse the emission spectra, it seems more justified to use the cross section for the excitation of level ($C\,^3\Pi_u$, $v = 0$) calculated from the emission cross sections.

3.2.2. Excitation cross section of N_2^+ ($B\,^2\Sigma_u^+$, $v' = 0$) from ground state N_2 molecules. The excitation cross section of level N_2^+ ($B\,^2\Sigma_u^+$) from ground state molecules $N_2(X\,^1\Sigma_g^+)$ was obtained in [40] by the method (e,2e).

However, Doering and Yang [42] suggested that, in order to get an adequate cross section there should be a compromise between the technique (e,2e) and the emission measurements. From their (e,2e) results and previous optical experiments, they determined the best value for σ^{Emis}, from which the excitation cross section can be derived.

The emission cross section (0.0) at 391.44 nm was measured in [39], but the results should be renormalized to the best value established in [40], at 100 eV. This means the cross sections from [39] must be multiplied by 0.871. The final result constitutes the excitation cross section σ_X^{B+} recommended in [28] and used in this study and it is shown in dashed lines in figure 2.

3.2.3. Excitation cross section of N_2^+ ($B\,^2\Sigma_u^+$, $v' = 0$) from ground state N_2^+ ions. The last cross section required to apply the diagnostic method proposed in this paper corresponds to the process $e + N_2^+(X\,^2\Sigma_g^+, v = 0) \to e + N_2^+(B\,^2\Sigma_u^+, v' = 0)$. Crandall *et al* [43] determined it from the emission cross section. As shown in [44], the cross section from [43] is in good agreement with the measurements reported in [45]. An interpolation to these data through an analytic expression is available in [29], and is taken here. The corresponding cross section, σ_{X+}^{B+}, is represented by the dotted line in figure 2.

4. Model discussion

In order to define well the domain of validity of the method being suggested to determine the electron temperature and density from OES measurements, three of the assumptions enunciated in section 3 deserve careful consideration, namely, the possible influence on the results of the formation of $N_2(C\,^3\Pi_u)$ from the reactions involving $N_2(A\,^3\Sigma_u^+)$ metastables, the plausible existence of a vibrationally excited distribution of $N_2(X\,^1\Sigma_g^+)$ molecules, and the eventual presence of a non-Maxwellian EEDF. They are discussed separately below.

4.1. Non-Maxwellian EEDF

In principle, the restriction of considering a Maxwellian EEDF is not very critical. Evidently, it considerably simplifies the calculation of the relevant electron impact excitation rate coefficients but, if necessary, a Boltzmann solver can be used to obtain these coefficients. However, this is a rather academic point of view, since the EEDF is not only a function of the average electron energy (or of the reduced electric field), as it strongly depends on the vibrational temperature of ground state $N_2(X\,^1\Sigma_g^+)$ molecules [46]. Therefore, in practice, a non-Maxwellian EEDF may markedly complicate the application of the procedure.

Interestingly enough, our Langmuir probe measurements indicate that under the present working conditions the EEDF is in fact non-Maxwellian. Bear in mind that one possibility to get a better description of the EEDF and to improve the method when the EEDF strongly deviates from a Maxwellian is to consider an EEDF with the form suggested in [18]. In the case of molecular nitrogen, a sum of two functions $f = k_1 f_1 + k_2 f_2$ was proposed, where f_1 describes the low-energy part of the EEDF $f(\varepsilon)$, while f_2 describes the high-energy part. Only the electrons in the tail of the distribution have enough energy to excite N_2 or N_2^+. Thus, only f_2 is important for the calculation of the electron rate coefficients $\langle\sigma v_e\rangle$ in equations (10) and (11). Note that the agreement observed in the results for n_e by both techniques (cf figure 7) is only possible if f_2 is nearly Maxwellian. This justifies why the suggested diagnostic technique yields very good results and can be applied, even if one of its basic assumptions in rigor fails. A detailed analysis of the question will be conducted in a subsequent publication.

4.2. Vibrational distribution of the electronic state $N_2(X\,^1\Sigma_g^+)$

It is interesting to examine the hypothesis that the predominant species is the molecules in the ground state $N_2(X\,^1\Sigma_g^+, v = 0)$. The vibrational distribution function (VDF) of $N_2(X\,^1\Sigma_g^+)$ molecules can be determined as detailed in [24], where it is assumed that the collisions between electrons and molecules satisfy the adiabatic approximation. In this case, it is possible to map the VDF of ground state $N_2(X)$ molecules from the

VDF of excited $N_2(C)$ molecules simply through the Franck–Condon factors. Under the conditions of this study, from the relative population of $N_2(C\,^3\Sigma_u, v)$, obtained by OES, it is concluded that about 90% of the neutral molecules are in the state $v = 0$.

Another interesting point worth emphasizing is that the ratios of the emission intensities from the different vibrational levels of $N_2(C\,^3\Sigma_u)$ are approximately constant when the discharge parameters (such as pressure, discharge current, gas flow, etc) are changed. This means that the assumption can bring a shift in all the calculations, but the behaviour will not be affected when the discharge operating conditions are changed. Therefore, the relative results are always correct and an independent normalization allows a consistent determination of the absolute values.

A similar situation occurs concerning the VDF of $N_2^+(X\,^2\Sigma_g^+)$ ions. However, taking into account (11), a bigger error than merely a shift in the results may be made if processes (8) and (9) have comparable contributions to the formation of $N_2^+(B\,^2\Sigma_u^+, v' = 0)$ excited ions.

4.3. Effect of the metastable state $N_2(A\,^3\Sigma_u^+)$

As is well known [22], excitation from metastable states may increase the population of the radiative states. Two possible reactions forming the level $C\,^3\Pi_u$ from the metastable state $A\,^3\Sigma_u^+$ are

$$N_2(A) + N_2(A) \rightarrow N_2(C) + N_2(X), \tag{12}$$

$$e + N_2(A) \rightarrow e + N_2(C). \tag{13}$$

The rate coefficient of the pooling reaction (12) is $k = 1.5 \times 10^{-10}\,\mathrm{cm^{-3}\,s^{-1}}$ [47], whereas the rate coefficient of process (13) depends on the EEDF. Both processes have been considered in [22]. The cross section for electron stepwise excitation is given in [48], where the corresponding rate coefficient is calculated for the case of a Maxwellian distribution. For an electron temperature in the plasma of the order of 1 eV, the reaction rate is $\sim 10^{-11}\,\mathrm{cm^3\,s^{-1}}$.

As shown in [24, 47], if the pooling reaction (12) is preponderant, it produces an overpopulation of the level $N_2(C\,^3\Pi_u, v = 1)$. This overpopulation in $v = 1$ is not observed in our measurements, giving an *a posteriori* confirmation that the pooling reaction does not contribute significantly to the production of the $N_2(C\,^3\Pi_u)$ state.

Clearly, by taking into account the corresponding rate coefficients, process (13) only has a larger contribution to the formation of $N_2(C\,^3\Pi_u)$ molecules than (12) if the ionization degree is higher than the relative population of $N_2(A\,^3\Sigma_u^+)$ metastables. For the conditions under study the ionization degree is lower than $\sim 1.5 \times 10^{-5}$ (see section 5), which means reaction (13) can only have a significantly higher rate than (12) if $[N_2(A)]/n_0 \ll 1.5 \times 10^{-5}$, where $[N_2(A)]$ is the density of $N_2(A\,^3\Sigma_u^+)$ and n_0 is the gas density. This looks unlikely, as shown from the calculations in [22]. Furthermore, for electron energies of about 1 eV the rate coefficient for direct excitation of $N_2(C\,^3\Pi_u)$ from $N_2(X\,^1\Sigma_g^+)$ is of the order 10^{-12}–$5 \times 10^{-10}\,\mathrm{cm^3\,s^{-1}}$ [46], which readily eliminates reaction (13) as an important source of $N_2(C\,^3\Pi_u)$ molecules.

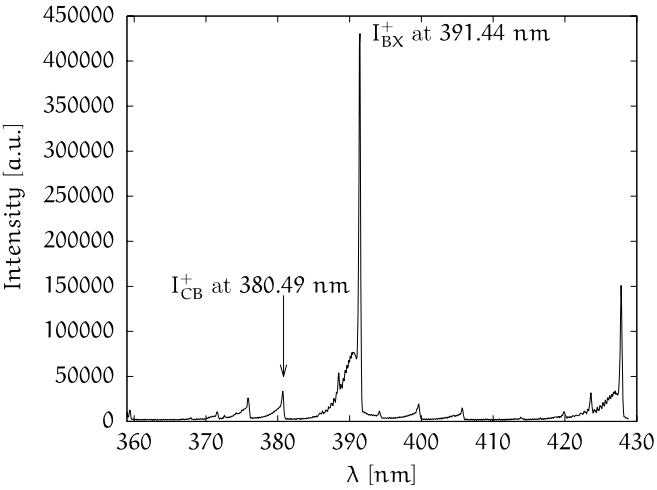

Figure 3. Emission spectrum with the two bands of interest in this work: pressure 3.80 Torr, cathode voltage −630 V, discharge current 0.85 A and position h_1.

5. Results

In compliance with sections 2 and 3, the emission intensities I_{BX}^+ at 391.44 nm and I_{CB} at 380.49 nm were measured in two different positions in the chamber, $h_1 = 6$ mm and $h_2 = 18$ mm (cf figure 1). A typical spectrum from our experiments is reproduced in figure 3. Langmuir probe measurements were additionally carried out for the same positions. The gas pressure varied in the range 2–4 Torr. Details on the estimation of the error bars shown in figures 4–8 are given in section 5.1.

Figures 4 and 5 show the emission intensities I_{BX}^+ and I_{CB} measured at the two different positions. According to the discussion in section 3, these are the intensities required to use the OES diagnostic method proposed in this paper. They allow the determination of the absolute values of n_e and T_e, as long as one value of n_e or T_e is provided for calibration at a specific condition. In this work such calibration is given by the Langmuir probe measurements, and we have chosen the value of n_e at $p = 2$ Torr and position h_2 as the calibration point. In h_1 both intensities increase with pressure, simply reflecting the increase in the densities of N_2 molecules and N_2^+ ions, the electron temperature not changing significantly in this range (see figure 9). On the other hand, in h_2 both intensities decrease when the pressure increases, following the decrease in n_e (equal to N_2^+ due to charge neutrality), see figure 7.

Keep in mind that if an independent determination of n_e or T_e is not possible, the technique can be employed to determine qualitative variation of T_e and the n_e. In that case, in practice it is interesting to analyse the ratio I_{BX}^+/I_{BC}, in a procedure bearing similarities to proposals by other authors [16, 23, 26]. In fact, if process (8) is clearly dominant over (9) in populating $N_2^+(B\,^2\Sigma_u^+, v' = 0)$, then I_{BX}^+/I_{BC} even provides the absolute value of T_e and the relative dependence of n_e [16]. The ratio I_{BX}^+/I_{BC} is depicted in figure 6. It decreases with gas pressure, which reflects the expected decrease in the ionization degree in this pressure range (confirmed in figure 8).

Figure 7 exhibits the OES and Langmuir probe measurements of the electron density. The agreement between

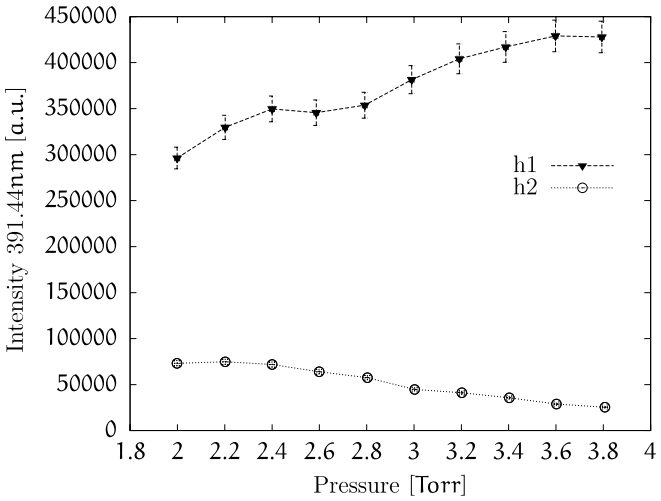

Figure 4. Emission intensity I^{+}_{BX} at 391.44 nm as a function of pressure at positions h_1 and h_2.

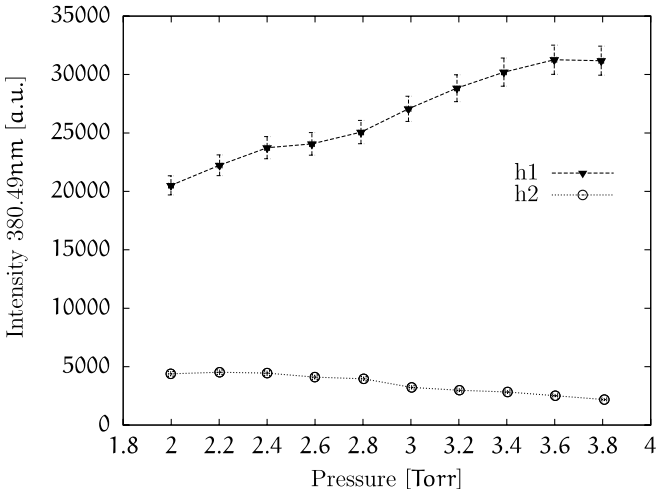

Figure 5. Emission intensity I_{CB} at 380.49 nm as a function of pressure at positions h_1 and h_2.

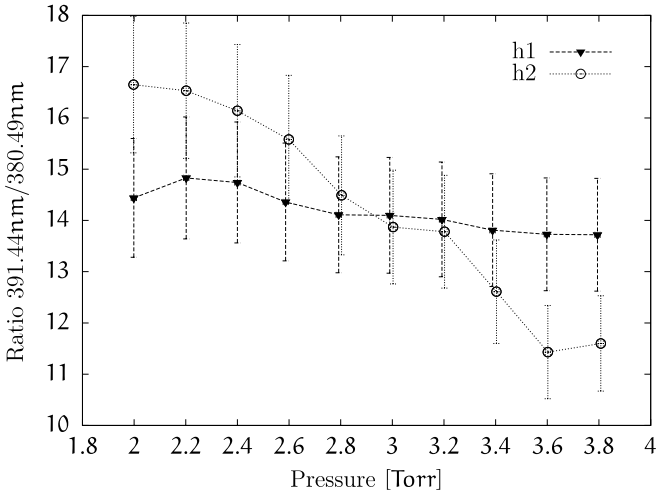

Figure 6. Variation of the ratio I^{+}_{BX}/I_{BC} with pressure, for the two positions h_1 and h_2.

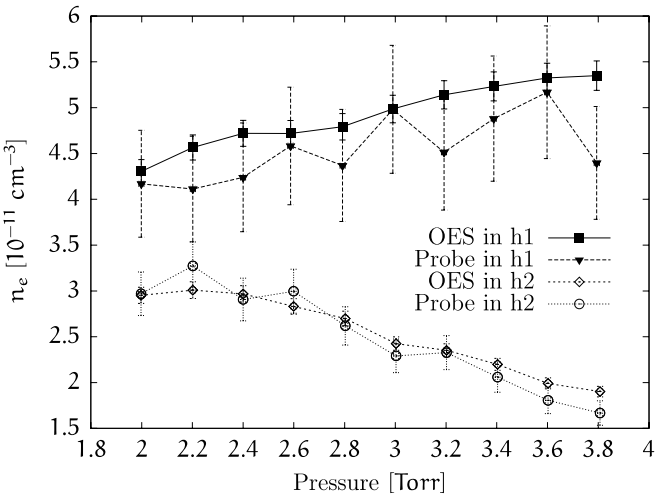

Figure 7. Electron density as a function of pressure for the two positions h_1 and h_2, determined from the new OES procedure and from the Langmuir probe measurements. Results were calibrated at $p = 2$ Torr in position h_2.

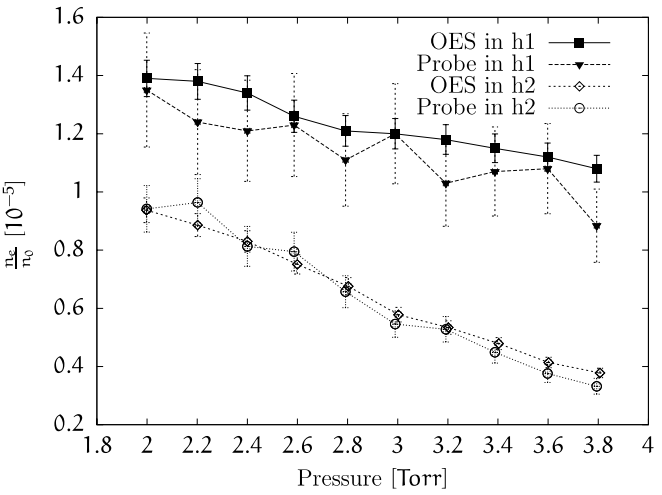

Figure 8. Variation of the ionization degree with pressure, for the two positions h_1 and h_2.

both procedures is excellent, validating the applicability of the new approach to determine the electron density proposed in this work. The corresponding ionization degrees are represented in figure 8, corroborating the results from figure 6.

The electron temperatures determined by the two methods are plotted in figure 9. Closer to the cathode, at position h_1, both methods provide similar results. However, at h_2 there is a significant disagreement, the probe measurements yielding much lower values of T_e. This is essentially a consequence of the presence of a non-Maxwellian EEDF. As a matter of fact, the probe measurement corresponds to average electrons, which have a relatively low energy. In turn, T_e measurements with OES reflect only the electrons in the tail of the distribution. More precisely, the OES result provides an effective temperature of the electrons with energies above the excitation and ionization thresholds.

Actually, since the EEDF is non-Maxwellian the two diagnostic techniques scan two different groups of electrons.

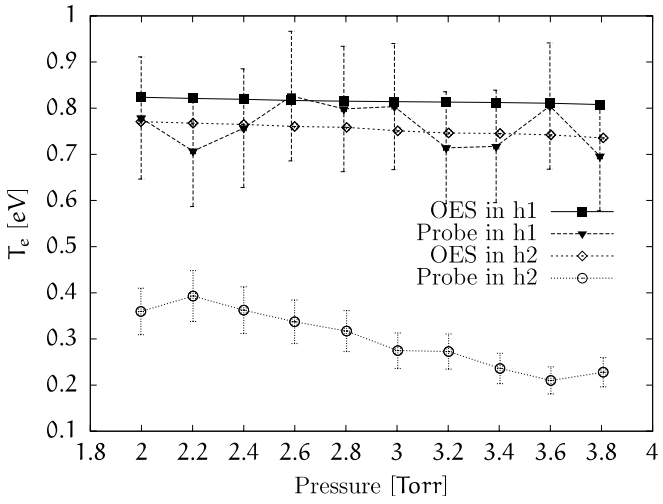

Figure 9. Electron temperature as a function of pressure for the two positions h_1 and h_2, determined from the new OES procedure and from the Langmuir probe measurements.

Therefore, the agreement in h_1 and the disagreement in h_2 are rather formal, as the measurements characterize distinct parts of the EEDF. As referred to in section 4, in order to achieve a better description of their distribution one should use an EEDF with the form proposed in [18]. We pursue our investigation in this direction, and the results will be reported in the near future. Nonetheless, keep in mind that these remarks about T_e do not influence the determination of the electron density. Thus, the comparison presented in figures 7 and 8 for n_e and the ionization degree is always valid, which confirms the correctness of our approach.

Finally, it is interesting to analyse which of the two reactions (8) and (9) has an higher importance in the excitation of $N_2^+(B, v = 0)$ [16, 18, 19]. By using the values of T_e and n_e already determined, it is immediate to evaluate the contribution of each mechanism to the emission intensity of the I_{BX}^+ band at 391.4 nm. For the present working conditions, process (9) clearly dominates over (8). Therefore, the scheme proposed in [16] cannot be applicable here.

5.1. Error estimation

This section describes in detail how the error bars presented in the previous figures were estimated.

In the OES measurements the error was estimated by measuring the maximum fluctuation of the band head intensities for several measurements in identical discharge conditions (same pressure, voltage, flow, etc). This fluctuation was in all cases less than 4%, therefore this value was adopted to estimate the uncertainty in the band heads. Because of the simplicity of the equations of the method developed in this work, we can calculate the uncertainty produced by these fluctuations in n_e to be less than 3%, whereas in T_e it is only about 0.5%.

Of course the values above are measurement errors, not eventual uncertainties associated with the validity of the method. Another possible source of errors is related to the cross sections used, so it is important to choose them carefully, as thoroughly discussed in section 3.2. Although, it is interesting to observe that if the cross sections only differ by a multiplicative constant and the process (8) is negligible, as in our case, then this difference will not affect the calculations of n_e and T_e, because the method uses a calibration point.

In what concerns the probe measurements, and as it was described in section 2, each point of the probe characteristic curve is obtained averaging 200 measurements in the current and 20 measurements in the voltage, which considerably reduces the characteristic noise. Despite this fact, in order to obtain the EEDF it is necessary to use a smoothing method on the probe characteristic. For this purpose, we used a cubic spline smoothing [49]. It was observed that the fluctuations in the values of n_e are always lower than 14% and 8%, respectively, in h_1 and h_2. The fluctuations in the values of T_e are always below 17% in h_1 and 14% in h_2. The higher uncertainty in h_1 is due to the larger fluctuations of the plasma near the cathode, which produces a bigger dispersion of the probe characteristic points. This is increased by the successive derivatives, causing the observed uncertainties in the value of T_e and n_e. Note as well that when the EEDF is non-Maxwellian the only correct method for calculating n_e and T_e from the probe is through equations (5) and (6).

Finally, keep in mind that in order to compare both techniques measurements must be made exactly the same distance above the cathode, since n_e and T_e are significantly dependent on height, as can be seen in figures 7 and 9.

6. Conclusions

In this work we have proposed a new method to experimentally determine the electron temperature, T_e, and electron density, n_e, in the negative glow of a nitrogen pulsed discharge operating at pressures $p = 2$–4 Torr. The technique is based on OES, and involves the measurement of the emission intensities of the first negative I_{BX}^+ (0, 0) bands at 391.44 nm and the second positive I_{BC} (0, 2) bands at 380.40 nm. The procedure allows the absolute determination of n_e and T_e, as long as one calibration point for n_e (or T_e) is provided. If this is not possible, the method can still be used to obtain the qualitative dependence of T_e and the n_e.

The diagnostic method was tested and validated from its comparison with Langmuir probe measurements. For the n_e measurements, the agreement between both techniques was excellent, confirming its applicability and usefulness. For the conditions of this study,the electron densities varied in the range $(1.5–5.5) \times 10^{11}$ cm^{-3}. The ionization degree consistently decreases with increasing gas pressure, as a result of the increase in the electron–neutral collision frequency.

Our method rests on several assumptions which may limit its pertinence when used in different working conditions. The most critical one seems to be the hypothesis that the EEDF is Maxwellian. Indeed, a non-Maxwellian EEDF implies that OES measurements reflect only the temperature of the high-energy tail of the EEDF. Thus, OES measurements provide in fact an effective temperature of the electrons with energies above the ionization and excitation thresholds. In

turn, the temperatures deduced from the probe measurements correspond to the average electrons.

In principle, the method can be used at various other discharge conditions, as long as its assumptions remain valid. Lowering the gas pressure should not affect the validity of the diagnostics, as no additional heavy-particle kinetics would become important and the associated increase in the ionization degree would bring the EEDF closer to a Maxwellian. However, adding other gases into nitrogen would certainly require a reformulation of the procedure.Work is now in progress to better characterize the domain of validity of the new scheme, as well as to elucidate how to handle the cases where the EEDF deviates from a Maxwellian distribution.

Acknowledgments

The authors would like to thank Ing. Aldo Marenzana for this valuable collaboration in the development of the instrumentation. They thank Michael O Thompson of Cornell University for their help and support in using your program Genplot (www.genplot.com). They express grateful acknowledgment to Conicet (Argentina) and to the 'Agencia Nacional de Promoción Científica y Tecnológica' (National Agency for Scientific and Technologic Promotion), Argentina, PICT 12-13628/12-01981 and Josefina Prats Fundation.

References

[1] Maliska A M, de Oliveira A M, Klein A N and Muzart J L R 2001 Surface porosity sealing effect of plasma nitrocarburizing on sintered unalloyed iron *Surf. Coat. Technol.* **141** 128–34

[2] Stefanović I, Bibinov N K, Deryugin A A, Vinogradov I P, Napartovich A P and Wiesemann K 2001 Kinetics of ozone and nitric oxides in dielectric barrier discharges in O_2/NO_x and $N_2/O_2/NO_x$ mixtures *Plasma Sources Sci. Technol.* **10** 406–16

[3] Cheng Z, Li C X, Dong H and Bell T 2005 Low temperature plasma nitrocarburising of AISI 316 austenitic stainless steel *Surf. Coat. Technol.* **191** 195–200

[4] Baeva M, Gier H, Pott A, Uhlenbusch J, Höschele J and Steinwandel J 2002 Pulsed microwave discharge at atmospheric pressure for NO_x decomposition pulsed microwave discharge at atmospheric pressure for nodecomposition *Plasma Sources Sci. Technol.* **11** 1–9

[5] Rousseau A, Dantier A, Gatilova L, Ionikh Y, Röpcke J R and Tolmachev Y 2005 On NO_x production and volatile organic compound removal in a pulsed microwave discharge in air *Plasma Sources Sci. Technol.* **14** 70–5

[6] Villeger S, Cousty S, Ricard A and Sixou M 2003 Sterilization of *E. coli* bacterium in a flowing N_2–O_2 post-discharge reactor *J. Phys D: Appl. Phys.* **36** L60–2

[7] Pintassilgo C D, Kutasi K and Loureiro J 2007 Modelling of a low-pressure N_2–O_2 discharge and post-discharge reactor for plasma sterilization *Plasma Sources Sci. Technol.* **16** S115–22

[8] Coitout H and Cernogora G 2006 Experimental study of the temporal evolution of $N_2(C\,^3\Pi_u)$ and $N_2(B\,^3\Pi_g)$ in a nitrogen pulsed discharge *J. Phys. D: Appl. Phys.* **39** 1821–9

[9] Deepthi H C, Rajam B and Barshilia K S 2008 Growth and characterization of aluminum nitride coatings prepared by pulsed-direct current reactive unbalanced magnetron sputtering *Thin Solid Films* **516** 4168–74

[10] Qayyum A, Shaista Z, Shujaat A, Waheed A and Zakaullah M 2005 Optical emission spectroscopy of abnormal glow region in nitrogen plasma *Plasma Chem. Plasma Process.* **25** 551–64

[11] Ricard A 1996 *Reactive Plasmas* (Paris, France: Societe/Francaise du Vide)

[12] Levaton J, Ricard A, Henriques J, Silva H R T and Amorim J 2006 Measurements of $N(^4S)$ absolite density in a 2.45 GHz surface wave discharge by optical emission spectroscopy *J. Phys. D: Appl. Phys.* **39** 3285–93

[13] Brühl S P, Russell M W, Gómez B J, Grigioni G, Feugeas J N and Ricard A 1997 A study by emission spectroscopy of the N_2 active species in pulsed dc discharges *J. Phys. D: Appl. Phys.* **30** 2917–22

[14] Sakamoto T, Matsuura H and Akatsuka H 2007 Spectroscopic study on the vibrational populations of N_2 $C\,^3\Pi$ and $B\,^3\Pi$ states in a microwave nitrogen discharge *J. Appl. Phys.* **101** 023307

[15] Hugon R, Fabry M and Henrion G 1996 The influence of the respective durations of the discharge and the afterglow on the reactivity of a dc pulsed plasma used for iron nitriding *J. Phys. D: Appl. Phys.* **29** 761–8

[16] Britun N, Gaillard M, Ricard A, Kim Y M, Kim K S and Han J G 2007 Determination of the vibrational, rotational and electronic temperatures in N_2 and Ar–N_2 discharges *J. Phys. D: Appl. Phys.* **40** 1022–9

[17] Ricard A and Touzeau M 1977 Excitation des ions N_2^+ dans des décharges rf *J. Physique* **38** 669–72

[18] Behringer K and Fantz U 1994 Spectroscopic diagnostic of glow discharge plasma with non-maxwellian electron energy distributions *J. Phys. D:Appl. Phys.* **27** 2128–35

[19] Gordiets B F, Ferreira C M, Guerra V, Loureiro J, Nahorny J, Pagnon D, Touzeau M and Vialle M 1995 Kinetic model of a low pressure N_2–O_2 flowing discharge *IEEE Trans. Plasma Sci.* **23** 750–68

[20] Henrion G, Fabry M, Hugon R and Bougdira J 1992 Spectroscopic investigation of a temporal post-discharge plasma iron nitridind *Plasma Sources Sci. Technol.* **1** 117–21

[21] Gómez B J, Brühl S P, Feugeas J N and Ricard A 1999 The time variations of N_2 active species in pulsed N_2–H_2 dc dischrges *J. Phys. D: Appl. Phys.* **32** 1239–42

[22] Guerra V, Sa P A and Loureiro J 2004 Kinetic modeling of low-pressure nitrogen discharges and post-discharges *Eur. Phys. J. Appl. Phys.* **28** 125–52

[23] Zhu X and Pu Y 2005 Determining the electron temperature in inductively coupled nitrogen plasmas by optical emission spectroscopy with molecular kinetic effects *Phys. Plasmas* **12** 103501

[24] Levaton J, Amorim J, Monna V, Nagai J and Ricard A 2004 A detailed discussion of the $N_2(C\,^3\Pi_u)$ and $N_2(X\,^1\Sigma_g^+)$ vibrational temperatures in N_2 glow discharges *Eur. Phys. J. Appl. Phys.* **26** 59–64

[25] Zhu X and Pu Y 2008 Using OES to determine electron temperature and density in low-pressure nitrogen and argon plasmas *Plasma Sources Sci. Technol.* **17** 024002

[26] Zhu X, Pu Y, Guo Z and Pu Y 2006 A novel method to determine electron density by optical emission spectroscopy in low-pressure nitrogen plasmas *Phys. Plasmas* **13** 123501

[27] Demidov V I, Ratynskaia S V and Rypdal K 2002 Electric probes for plasmas: The link between theory and instrument *Rev. Sci. Instrum.* **73** 3409–39

[28] Itikawa Y 2006 Cross sections for electron collision with nitrogen molecules *J. Phys. Chem. Ref. Data* **35** 31–53

[29] Tabata T, Shirai T, Sataka M and Kubo H 2006 Analytic cross sections for electron impact collisions with nitrogen molecules *At. Data Nucl. Data Tables* **92** 375–406

[30] Zubek M and King G C 1994 Differential cross sections for electron impact excitation of the $C\,^3\Pi_u$, $E\,^3\Sigma_g^+$ and $a''^1\,\Sigma_g^+$ states of N_2 *J. Phys. B: At. Mol. Opt. Phys.* **27** 2613–24
[31] Poparic G, Vicic M and Belic D S 1999 Vibrational excitation of the $C\,^3\Pi_u$ state of N_2 by electron impact *Chem. Phys.* **240** 283–9
[32] Trajmar S, Register D F and Chutjian A 1983 Electron scattering by molecules: II. Experimental methods and data *Phys. Rep.* **97** 219–356
[33] Campbell L, Brunger M J, Nolan A M, Kelly L J, Wedding A B, Harrison J, Teubner P J O, Cartwright D C and McLaughlin B 2001 Integral cross sections for electron impact excitation of electronic states of N_2 *J. Phys. B: At. Mol. Opt. Phys.* **34** 1185–99
[34] Ohmori Y, Shimozuma M and Tagashira H 1988 Boltzmann equation analysis of electron swarm behaviour in nitrogen *J. Phys. D: Appl. Phys.* **21** 724–9
[35] Itikawa Y (ed) 2003 *Photon and Electron Interactions with Atoms, Molecules and Ions* vol I/17/C (Berlin: Springer)
[36] Majeed T and Strickland D J 1997 New survey of electron impact cross sections for photoelectron and auroral electron energy loss calculations *J. Phys. Chem. Ref. Data* **26** 335–49
[37] Zubek M 1994 Excitation of the $C\,^3\Pi_u$ state of N_2 by electron impact in the near-threshold region *J. Phys. B: At. Mol. Opt. Phys.* **27** 573–81
[38] Shemansky D E, Ajello J M and Kanik I 1995 Electron excitation functions of the N_2 second positive system *Astrophys. J.* **452** 472–9
[39] Borst W L and Zipf E C 1970 Cross section for electron-impact excitation of the (0,0) first negative band of N_2^+ from threshold to 3 keV *Phys. Rev.* A **1** 834–40
[40] Doering J P and Yang J 1996 Comparison of the electron impact cross section for the N_2^+ first negative (0,0) band (λ3914 Å) measured by optical fluorescence, coincidence electron impact, and photoionization experiments *J. Geophys. Res.* **101** 19723–8
[41] Fons J T, Schappe R S and Lin C 1996 Electron-impact excitation of the second positive band system $C\,^3\Pi_u \rightarrow B\,^3\Pi_g$ and the $C\,^3\Pi_u$ electronic state of the nitrogen molecule *Phys. Rev.* A **53** 2239–47
[42] Doering J P and Yang J 1997 Direct experimental measurement of electron impact ionization-excitation branching ratios: III. branching ratios and cross sections for the $N_2^+(X\,^2\Sigma_g A\,^2\Pi_u$, and $B\,^2\Sigma_u)$ states at 100 eV *J. Geophys. Res.* **102** 9683
[43] Crandall D H, Kauppila W E W E, Phaneuf R A, Taylor P O and Dunn G H 1974 Absolute cross sections for electron-impact excitation of N_2^+ *Phys. Rev.* A **9** 2545–5
[44] Nagy A 2003 $X\,^2\Sigma_g^+(v''=0) \rightarrow B\,^2\Sigma_u^+(v'=0)$ excitation cross-sections of N_2^+ molecular ion by electron impact and the vibrational energy levels of the three target states $N_2^+(X\,^2\Sigma_g^+$, $A\,^2\Pi_u$ and $B\,^2\Sigma_u^+)$. *Chem. Phys.* **286** 109–14
[45] Dashchenko A I, Zapesochnyi I P and Imre A I 1973 Excitation cross-sections of bands of the first negative system of nitrogen in electron-ion collisions *Opt. Spectrosc.* **35** 562–4 (Engl. Transl.)
[46] Loureiro J and Ferreira C M 1986 Coupled electron energy and vibration distribution functions in stationary N_2 discharges *J. Phys. D: Appl. Phys.* **19** 17–35
[47] Piper L G 1988 State-to-state $N_2(A\,^3\Sigma_u^+)$ energy-pooling reactions: I. Formation of $N_2(C\,^3\Pi_u)$ and the Herman infrared system *J. Chem. Phys.* **88** 231–9
[48] Bacri J and Medani A 1982 Electron diatomic molecule weighted total cross section calculation *Physica B+C* **112** 101–18
[49] Reinsch C H 1967 Smoothing by spline functions *Numer. Math.* **10** 177–83